Received: 06 April 2023, Accepted: 25 April 2023

Original Research

Journal of Advanced Veterinary Research
(2023) Volume 13, Issue 3, 526-530

Estimation of the Time Since Death Based on the Post-mortem Histopathological Changes in a Rat Brain: An Observational Study

Amany T. Mohammed[1*], Ahmed Abdelfattah-Hassan[2], Samar Abdo[3], Maha I.M. Ali[4], Eman Wagih[1]

[1]Forensic Medicine and Toxicology Department, Faculty of Veterinary Medicine, Zagazig University 44511, Zagazig, Sharkia, Egypt.

[2]Anatomy and Embryology Department, Faculty of Veterinary Medicine, Zagazig University 44511, Zagazig, Sharkia, Egypt.

[3]Biochemistry Department, Faculty of Veterinary Medicine, Zagazig University 44511, Zagazig, Sharkia, Egypt.

[4]Forensic Medicine and Clinical Toxicology Department, Faculty of Medicine, Suez Canal University, 41522, Ismailia, Egypt.

***Correspondence**
Corresponding author:Amany T. Mohammed
E-mail address: Atkhalil@zu.edu.eg

Abstract

A comprehensive inference of the structural alterations that occur in the body after death plays a pivotal role in the accurate interpretation of the time since death in many human and animal death investigations. Particular estimation of post-mortem interval (PMI) is usually affected by many frequently changed environmental and other factors that influence the sequential changes that happen to a body after death. Histopathologic investigation in autopsy is a unique technique to investigate PMI. Moreover, it is a supplementary investigation in cases where macroscopic examinations fail to display a diagnostic pathology regarding death. Here, we investigated the post-mortem histopathological changes in rats' brains to pinpoint the time that elapsed since death. For this purpose, we used 72 male Sprague-Dawley rats divided into two main groups 36 young-aged rats and 36 adult-aged rats. The two main groups were subdivided into 6 subgroups (6 rats/subgroup). After accommodation, rats were cervically dislocated and intact brain was collected at 0-hour post-mortem and at the 2nd, 4th, 8th, 12th, and 24th h post-mortem at room temperature (RT) and 4°C. The histopathological changes of collected brain tissues revealed that the post-mortem changes begin to be emphasized after 8 h post-mortem in both young and adult rats at RT than at 4°C. Those changes included hemorrhage, mild neuronal degeneration, and apoptotic neurons that were prominent in the cerebral cortex. Moreover, cerebral cortex histopathologic changes continued till 24 h post-mortem. Also, the cerebellar changes followed the same path as the cerebral ones. However, the results deduced that the post-mortem changes were prominent at RT in young-aged rats. In conclusion, observation of the histopathological changes of brain tissue under certain individual and environmental circumstances can be an effective, inexpensive, and additional tool to accurately estimate the PMI.

KEYWORDS
PMI, Cerebrum, Cerebellum, Histopathological changes, Temperature, Age.

INTRODUCTION

Post-mortem interval (PMI) is the time elapsed after the death of a living organism until the official investigation of the deceased. Realizing the time since death or post-mortem interval is a crucial point for effective forensic pathology (Hunter et al., 2017). During this time, there are many complex and consecutive biochemical and pathological processes that are initiated to represent the proceeding of the body's decomposition (Brooks, 2016). Following death, the sequential alterations of the structure and composition of the deceased body proposed that the evaluation of the types and degrees of changes may enable the estimation of time since death (Ferreira and Cunha, 2013). A thorough understanding of the physical and chemical changes that occur in the body after death is crucial for accurate interpretation of gross and microscopic pathology at autopsy. Estimation of the PMI is remarkably important, as it can help investigate the possible causes of death (Cockle and Bell, 2015). The estimation of the PMI is important in many humans and is similarly relevant in some animal forensic investigations (Brooks, 2016). However, the rate of postmortem changes progression may be accelerated or even decelerated by various factors related to the organism and its surrounding environment (Perper, 2006). The postmortem process is by several factors including age, sex, and physical, and physiological state of the deceased, and makes the determination of PMI more complicated. Moreover, environmental temperature and humidity are external factors that also interfere with the accurate estimation of PMI (Elalfy et al., 2019).

The accuracy in the determination of the time since a death has not significantly improved because of those factors (Sutherland et al., 2013). Although most studies of changes in the organs' morphology during PMI have concentrated on gross anatomy, some researchers have detailed predictable changes in microanatomy or ultra-structural changes in cellular architecture (Bryant and Boekelheide, 2007). Previous studies observed some histologic changes in dogs at various postmortem time intervals. The changes ranged from the greatest microscopic changes in the heart, liver, lung, pancreas, tonsil, thyroid, and urinary bladder with increasing time after death (Erlandsson and Munro, 2007). Whilst these microscopic tissue changes alone can't be a reasonable clue in the estimation of PMI, these notions may be carried out to other tissues and may be used to provide ancillary

ISSN: 2090-6277/2090-6269/

supporting evidence in some cases (Brooks, 2016). Unfortunately, there is a scarcity of studies that investigate PMI through tissue morphology and microscopic changes in brain tissue. Wherefore, the goal of this study was to investigate the early structural post-mortem changes using a routine histopathologic examination and quantitative analysis to obtain an accurate diagnosis of PMI in the young and adult rat's brains at 0-hour, and 2nd, 4th, 8th, 12th, and 24th-hour postmortem (hpm) at low and room temperatures.

MATERIALS AND METHODS

Animals

The laboratory animal unit of the Faculty of Veterinary Medicine, Zagazig University, Egypt provided 36 healthy adult (3 months old) and 36 young (6 weeks old) male Sprague-Dawley rats weighing 150-180 and 80-90 g respectively. Animals were kept in standard hygienic conditions at the experimental animal center for five days before the collection of brain tissue samples. All animals were exposed to a normal light/dark cycle and room temperature (23±2°C).

Ethical Statement

Before conducting this experiment, the study protocol was approved by the institutional animal care and use committee, Zagazig University. by the ethical approval number: ZU-IACUC/2/F/437/2022,

Experimental design

A total of 36 adult male Sprague-Dawley rats were randomly dispensed into six groups (6 rats each). The same was carried out regarding young male rats where a total of 36 young male Sprague-Dawley rats were also randomly distributed into another six groups. The control groups (G1A) for adult rats and (G1Y) for the young ones that were sacrificed by cervical dislocation and the brain tissues were taken immediately after death (0- hour). The G2, G3, G4, G5, and G6 for both young and adult animals were also cervical dislocated, and the whole brain was taken at the 2nd, 4th, 8th, 12th, and 24th hpm, respectively. Humane endpoint criteria for euthanasia were applied to all animals where there wasn't any unexpected distress or pain. Brain specimens were collected from all rats at a certain time frame of the experiment (at room temperature RT 25°C and 4°C) for the estimation of cellular changes in the brain tissue.

The collected specimens from Brain tissues were fixed in 10% neutral buffered formalin for 24 h, dehydrated in graded ethanol, cleared in xylene, embedded in paraffin, sectioned at 5 µm thick tissue sections, stained with hematoxylin and eosin (H&E), and examined microscopically for any histopathological alterations (Suvarna et al., 2018). Each slide was examined for cerebral and cerebellar alterations along the defined time post-mortem in both young and adult rats at RT and 4°C. All images were taken by a microscope (Leica) DM750 connected to a digital camera in the Anatomy Department, Faculty of Veterinary Medicine, Zagazig University, Zagazig. Egypt.

RESULTS

Histopathological findings

Young-aged animal group

Cerebral cortex findings

Light microscopic examination of the hematoxylin and eosin (H&E) stained sections of the cerebral cortex at the 0-hour till 4 hpm at RT and at 4°C showed normal histological architectures of neurons, glia cells, vasculatures, and neuropil (it is any area in the nervous system composed of mostly unmyelinated axons, dendrites, and glial cell processes that form a synaptically dense region containing a relatively low number of cell bodies) (Fig. 1A-1C and Fig. 1G-1I). The morphological changes initiated at 8h post-mortem at RT exhibited hemorrhage, and mild neuronal degeneration (Fig. 1D). However, the cerebral cortex at 8 h post-mortem at 4°C revealed dilated blood vessels, normal neurons, and supporting cells (Fig. 1J). While, at the 12th post-mortem, there was an increased number of apoptotic neurons with

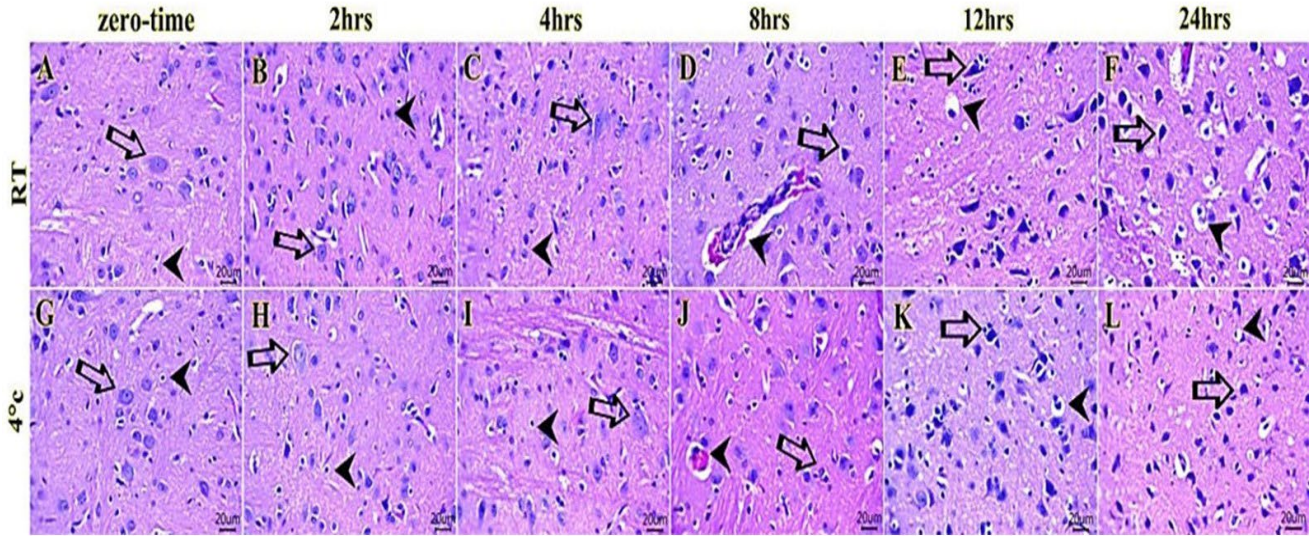

Fig. 1. Representative photomicrographs of H&E-stained sections from cerebral cortex showing normal histological architectures of neurons (arrows), glia cells (arrowheads), and neuropil from the 0-time to 4 h post-mortem at RT (A to C) and 4°C (G to I). In an 8 h post-mortem, there are hemorrhages (arrowhead), mild neuronal degeneration (arrow) at RT. as well, dilated blood vessels (arrowhead), normal neurons (arrow), and supporting cells at 4°C. In addition, an increased number of apoptotic neurons (arrows) with pyknotic nuclei, satellitosis, and vacuolated neuropil (arrowheads) in 12 h post-mortem in RT (E) than at 4°C (K). After 24 h, there are neuron degenerations (arrows), perineuronal vacuolations (arrowheads), and perivascular edema at RT (F) than at 4°C (L). Scale bar (20 µm).

pyknotic nuclei, satellitosis, and vacuolated neuropil detected in RT (Fig. 1E) than in 4°C (Fig. 1K). Furthermore, there is neuronal degeneration, perineuronal vacuolations, and perivascular edema at 24 hpm, were more pronounced at RT (Fig. 1F) when compared to 4°C (Fig. 1L).

Cerebellum findings

Light microscopic examination of the H&E stained sections of the cerebellum displayed normal histological structures of the molecular layer, Purkinje cell layer, and granular layer in groups 0-hour to 4 h post-mortem at RT and 4°C (Fig. 2A-2C and Fig. 2G-2I). Concerning 8 h post-mortem, at both RT (Fig. 2D) and at 4°C (Fig. 2J), there were vacuolations and apoptosis in the Purkinje cell layer. Moderately apoptotic Purkinje cells were detected at 12 h post-mortem at both RT (Fig. 2E) and 4°C (Fig. 2K). Furthermore, some necrotic Purkinje cells, granular cells, and vacuolated molecular layer were commonly seen at 24 h post-mortem at RT (Fig. 2F), while fewer necrotic cells and vacuoles were observed at 4°C (Fig. 2L) compared to RT.

Adult-aged rat group

Cerebral cortex findings

Light microscopic examination of the H&E stained sections of the cerebral cortex showed normal histologic architectures of nerve cell bodies, the surrounding supported cells, and neuropil in all taken specimens from 0-time to 4 h post-mortem (Fig. 3A-3C and Fig. 3G-3I). In RT, the apoptotic neurons begin to appear at 8 h from death (Fig. 3D). Obvious satellitosis increased at 12 h after death indicating prominent post-mortem changes began

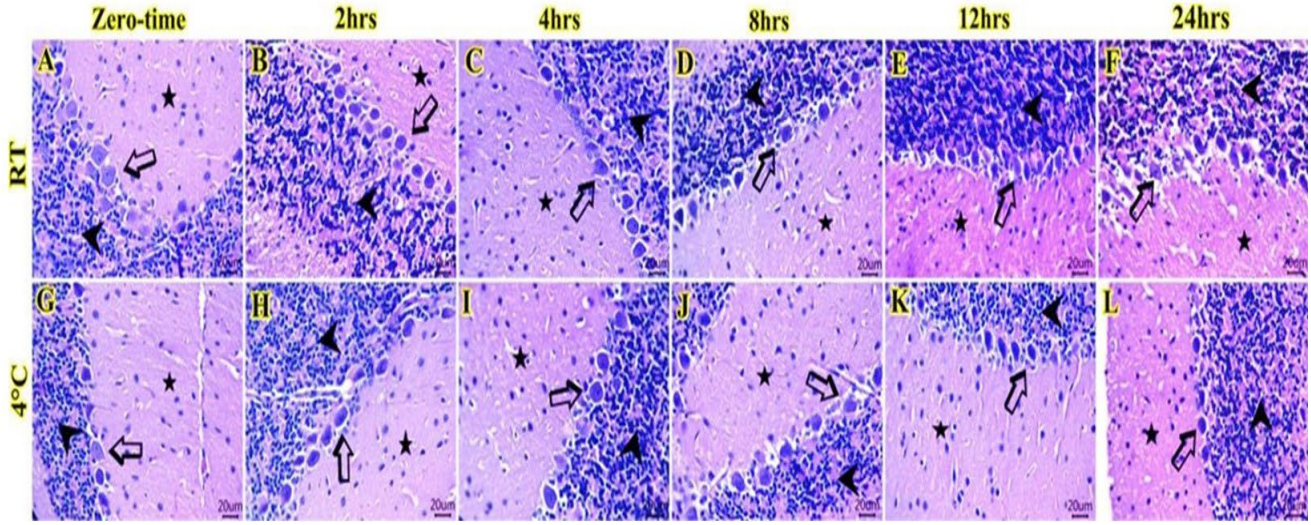

Fig. 2. Representative photomicrograph of H&E-stained Cerebellum sections showing normal histological structures of the molecular layer (stars), Purkinje cell layer (arrows), and granular layer (arrowhead) in groups zero-time to 4 h after death at RT (A-C) and at 4°C (G-I). In an 8 h postmortem, at both RT (D) and at 4°C (J), there were vacuolations, and apoptosis in the Purkinje cell layer (arrows). Moderate apoptotic Purkinje cells (arrows) appeared after 12 h at both RT (E) and at 4°C (K). Furthermore, some necrotic Purkinje cells (arrows) granular cells and vacuolated molecular layer after 24 h were seen more at RT (F) than at 4°C (L). Scale bar 20 μm.

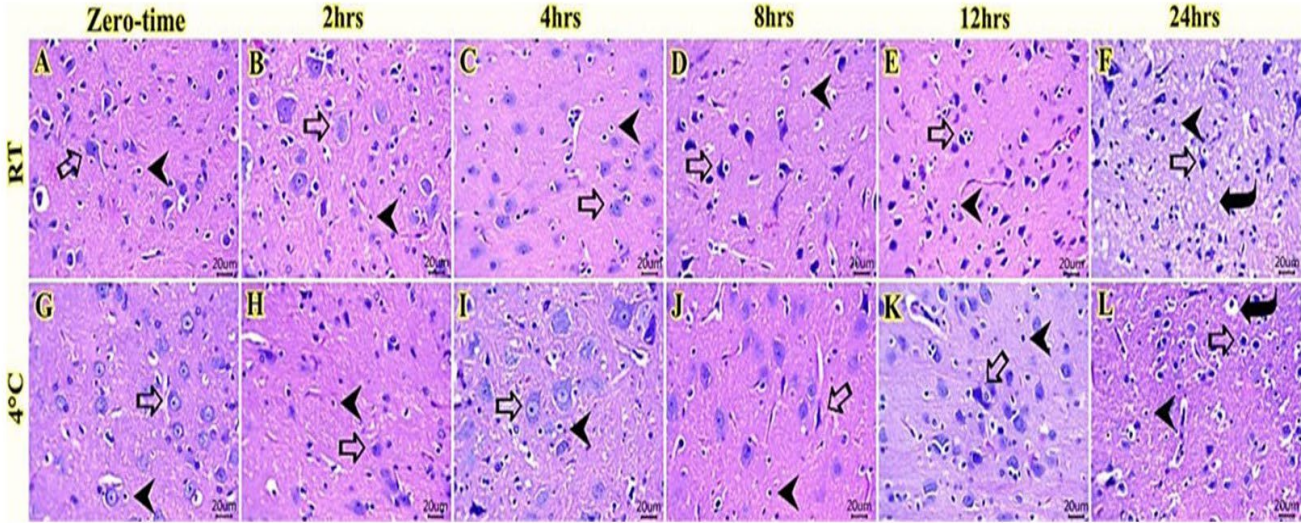

Fig. 3. Representative photomicrograph of H&E-stained sections from cerebral cortex showing normal histological structures of nerve cell bodies (arrows), surrounding supported cells (arrowheads), and neuropil from the zero-time to 4 h postmortem at RT (A to C) and 4°C (G to I). At RT the sections from 8 h postmortem, there are apoptotic neurons (arrow) (D) with increased satellitosis (arrow) at 12 h after death (E), as well, as moderately vacuolated neuropil (curved arrow) and apoptotic neurons (arrow) were seen at 24 h after death (F). At 4°C, at 8 h (J) and 12 h (K) after death, there are fewer apoptotic neurons (arrows). In addition, less vacuolated neuropil (curved arrow) was seen 24 h after death. Scale bar (20 μm).

to appear at this definite time (Fig. 3E). Additionally, moderate vacuolation of the neuropil and apoptotic neurons were the most eminent morphological and structural changes at 24 h post-mortem (Fig. 3F). Whereas, at 4°C and 8 h (Fig. 3J) and 12 h (Fig. 3K) post-mortem, there were less apoptotic neurons. In addition to less vacuolated neuropil at 24 h after death (Fig. 3L) when compared to RT groups.

Cerebellum findings

Cerebellum showed normal histological structures of the outer molecular layer, middle Purkinje cell layer, and inner granular layer in all specimens from 0-time to 8 h after death (Fig. 4A-4D and Fig. 6G-6J). In RT, the apoptotic and degenerated Purkinje cells were seen in few numbers at 12 h after death (Fig. 4E) and become numerous at 24 h after death (Fig. 4F). In 4°C, the samples at 12 h (Fig. 6K) and 24 h (Fig. 4L) after death, there was somewhat preserved structure of the 3 layers of cerebellum compared to the cerebellum of rats kept at RT.

DISCUSSION

The interpretation of PMI is a significant procedure in forensic investigations and has always been one of the primary goals of forensic medicine. The substantial morphologic and histologic changes that take place in the body after death were attributed to the cut-off of blood circulation and loss of regulatory mechanisms resulting in an enzymatic dissolution of the dead cells leading to cellular and nuclear degeneration. Various histo-morphologic analyses have been employed to identify the characteristic degenerative changes and determine the time elapsed after death in various soft tissues of the body including the brain, blood, skin, eyes, sebaceous gland, skeletal muscles, kidney, and liver. This diversity in methods helps to calculate the post-mortem interval (PMI) of an individual (Zdravković et al. 2006; Kushwaha et al. 2010; Pittner et al. 2016).

The purpose of the present work was to observe the histopathological changes in rat's brain during the early 24 hours after death (at 0-h, 2, 4, 8, 12, and 24 hpm) either at RT or at 4o C to conclude a presumptive method as a clue in PMI investigation and disclose whether or not a significant association between age and temperature of the cadaver could interfere with the PMI through time- and temperature- dependent histopathological changes. For this purpose, stained sections of the brain tissue of rats (cerebrum and cerebellum) were examined.

Putrefaction of the body after death is mainly affected by the circumstances of death, external environmental factors, and internal factors of the deceased (Gawande et al., 2012). The temperature and the bacterial load of the environment also affect the desiccation of the soft tissue. Based on that, our results showed that the most prominent changes in brain architecture began to appear through the first 8 h post-mortem and continue until 24 h in young-aged, cervical dislocated male rats kept at RT. Those alterations were concluded as hemorrhage, mild neuronal degeneration dilated blood vessels, increased number of apoptotic neurons with pyknotic nuclei, satellitosis and vacuolated neuropil neuronal degeneration, perineuronal vacuolations and perivascular edema in the cerebral tissue. On the other hand, brain tissue kept at 4o C showed less or normal histological structure. Moreover, the cerebellum of the same rats shows the same time-dependent changes sequence. Our results coincide with a previous study by Zaki et al. (2017) which deduced that the histopathological findings in the brain of cervical dislocated rats indicate brain tissue deterioration in conjunction with an increase in oxidant level and DNA fragmentation and a decrease in antioxidant levels. Such more prominent and severe histopathological alterations as neuronal shrinkage, with deep blue color, were the predominant findings.

After death, dead bodies were initially decomposed by autolytic enzymes and then progressed by putrefying bacteria that are activated at warm temperatures leading to degenerative changes which can be comprehended morphologically as well as histologically (Pittner et al. 2016). Little available literature was found about the histopathological alterations in the brain and evaluation at the time of death, but all studies were localized to other organs such as the kidney, muscles, liver, heart, and pancreas (Zaki et al., 2017). Furthermore, the histopathological alterations of our study on adult-aged cervical dislocated male rats declared that the apoptotic neurons begin to appear at 8 h from death with obvious satellitosis increased at 12 h after death indicating prominent post-mortem changes. In addition, moderate vacuolation of the neuropil related to the cerebrum was eminent at 24 h post-mortem. The series of histopathological changes were the same in a time-dependent manner in the cerebellar tissue where there were apoptotic and degenerated Purkinje cells were seen in few numbers at 12 h after death in samples kept at RT. However, the cerebrum and cerebellar tissue to some extent retained their

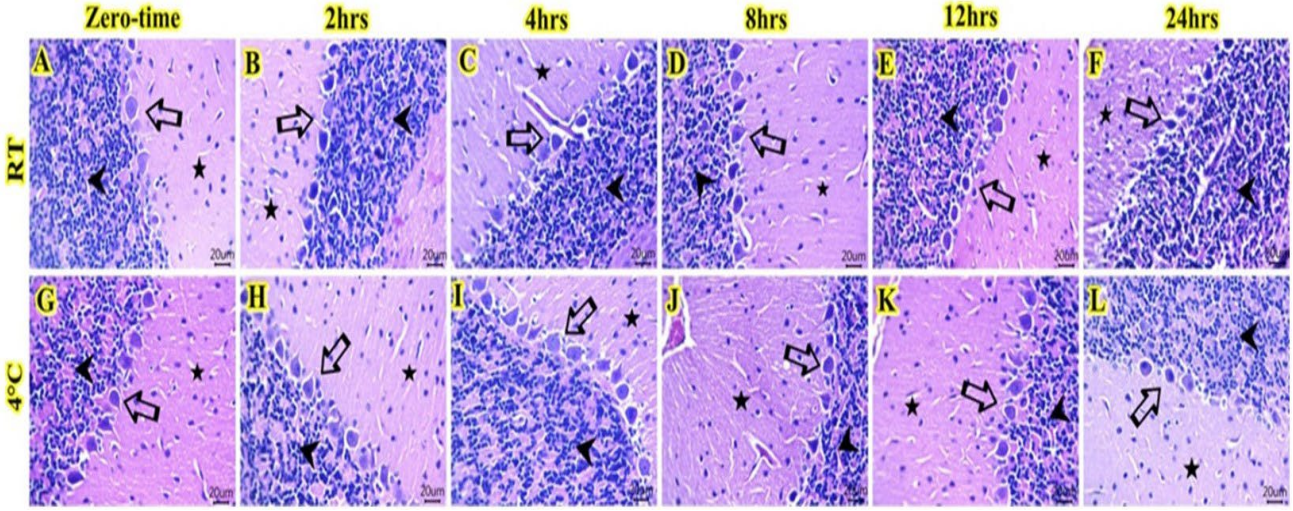

Fig. 4. Representative photomicrograph of H&E-stained Cerebellum sections showing normal histological structures of the outer molecular layer (stars), middle Purkinje cell layer (arrows), and inner granular layer (arrowhead) from 0-time to 8 h after death at RT (A-D) and 4°C (G-J). In RT, few numbers of apoptotic and degenerated Purkinje cells (arrow) were seen 12 h after death (E) and these become numerous (arrow) 24 h after death (F). At 4°C, cerebellar samples taken at 12 h (K) and 24 h (L) after death, showed preserved cerebellum structure. Scale bar 20 µm.

structure at 4°C at the specified time frame.

The process of autolysis (alterations in size, shape, electron density, and localization of cell structures) caused a sequential drop in the highly arranged structural organization of cells (De-Giorgio et al., 2019). The autolytic enzymes proved in lysosomes of living cells destroy their cell components after death. Those enzymes disintegrate intracellular material, including cell organelles, so the cytoplasm became homogenous with a loss of cell details (Hostiuc et al., 2017). This explains the results of the present study that showed the damage of brain (cerebrum and cerebellum) tissue in a time-dependent series of changes that are affected by the temperature and age of the deceased (environmental and individual factors).

CONCLUSION

Based on the obtained results and the previous studies we concluded that some environmental and individual factors can affect the estimated PMI. Also, the observation of the histopathological changes in the examined brain tissue can be an effective implement to designate the PMI. This study should be accepted as preliminary, and it requires confirmation with different blood samples in future studies, using gene expression markers to find out confirmatory results.

CONFLICT OF INTEREST

The authors declare that they have no conflict of interest.

REFERENCES

Brooks, J.W., 2016. Postmortem changes in animal carcasses and estimation of the postmortem interval. Vet. Pathol. 53, 929-940.

Bryant, B.H., Boekelheide, K., 2007. Time-dependent changes in post-mortem testis histopathology in the rat. Toxicol. Pathol. 35, 665-671.

Cockle, D.L., Bell, L.S., 2015. Human decomposition and the reliability of a Universal model for post-mortem interval estimations. Forensic Sci. Int. 253, 136.

De-Giorgio, F., Nardini, M., Foti, F., Minelli, E., Papi, M., d'Aloja, E., Ciasca, G. 2019. A novel method for post-mortem interval estimation based on tissue nano-mechanics. Int. J. Legal Med. 133, 1133-1139.

Elalfy, M.M., Ragheb, H.H., Hamed, M.F., Sleem, F.R., 2019. Biochemical markers and pathological features of postmortem time interval distinguishing freshwater and saltwater drowning induced death in albino rats. J. Sci. Tech. Res. 20, 14713-14719.

Erlandsson, M., Munro, R., 2007. Estimation of the post-mortem interval in beagle dogs. Sci. Justice. 47, 150-154.

Ferreira, M.T., Cunha, E., 2013. Can we infer post-mortem interval on the basis of decomposition rate? A case from a Portuguese cemetery. Forensic sci. Int. 226, 298-e1.

Gawande, M., Chaudhary, M., Das, A., 2012. Estimation of the time of death by evaluating histological changes in the pulp. Indian J. Forensic Med. Toxicol. 6, 80.

Hostiuc, S., Rusu, M.C., Manoiu, V.S., Vrapciu, A.D., Negoi, I., Popescu, M.V. 2017. Usefulness of ultrastructure studies for the estimation of the postmortem interval. A systematic review. Rom. J. Morphol. Embryol. 58, 377-384.

Hunter, M.C., Pozhitkov, A.E., Noble, P.A., 2017. Accurate predictions of postmortem interval using linear regression analyses of gene meter expression data. Forensic Sci. Int. 275, 90-101.

Kushwaha, V., Yadav, M., Srivastava, A.K., Agarwal, A., 2010. Time since death from degenerative changes in the Kidney. J. Indian Academy Forensic Med. 32, 37-41.

Perper, J.A., 2006. Chapter 3–Time of death and changes after death. Spitz and Fisher's Medicolegal Investigation of Death–Guidelines for the Application of Pathology to Crime Investigation. the 4th ed. Springfield: Charles C. Thomas, United States of America, pp. 87-127.

Pittner, S., Monticelli, F. C., Pfisterer, A., Zissler, A., Sänger, A.M., Stoiber, W., Steinbacher, P., 2016. Postmortem degradation of skeletal muscle proteins: a novel approach to determine the time since death. Int. J. Legal Med. 130, 421-431.

Sutherland, A., Myburgh, J., Steyn, M., Becker, P.J. 2013. The effect of body size on the rate of decomposition in a temperate region of South Africa. Forensic Sci. Int. 231, 257-262.

Suvarna, K.S., Layton, C., Bancroft, J.D., 2018. Bancroft's Theory and Practice of histological techniques E-Book. Elsevier Health Sciences.

Zaki, A.R., Tohamy, A.F., Yaseen, N.E.H., 2017. Estimation of postmortem intervals by some biochemical changes and DNA degradation in rat brain and skeletal muscle tissues. Mansoura J. Forensic Med. Clin. Toxicol. 25, 59-78.

Zdravković, M., Kostov, M., Stojanović, M., 2006. Identification of postmortem autolytic changes on the kidney tissue using PAS-stained method. Med. Biol. 13, 181-184.